Journal of Inorganic and General Chemistry
ZAAC
Zeitschrift für anorganische und allgemeine Chemie
DOI: 10.1002/zaac.201700096
ARTICLE

Synthesis, Characterization, and Photocatalytic Properties of Bismuth (III)-benzene-1,3,5-tricarboxylate

Fan Ye,[a] Zhi-Xian Wei,*[b] Jiang-Feng Song,*[a] Xu-Hong Wu,[a] and Pan Yue[b]

Abstract. $\{[Bi(BTC)(H_2O)_2]\cdot H_2O\}_n$ (H_3BTC = 1,3,5-benzenetricarboxylic acid) was synthesized by an eco-friendly hydrothermal method and characterized by single-crystal X-ray diffraction, IR and UV/Vis spectroscopy, photoluminescence (PL), and thermogravimetric analyses. The complex featured a 3D metal-organic framework with Bi_2 secondary building units. In the complex, the central Bi^{3+} is nine-coordinate, three central Bi atoms and three BTC^{3-} anions are interconnected into a ring with the dimension of 7.95×9.89 Å^2. Moreover, the complex is decomposed at over 388 °C, showing its highly thermal stability. Further, the complex exhibits photocatalytic activity for the degradation of methyl orange (MO) solution under UV light irradiation, and its structure can keep consistent with the original one after 9 h photocatalytic reaction, indicating that it is also very stable under UV light. Therefore, it could be anticipated the novel coordination complex will be a stable ultraviolet light catalyst.

Introduction

The photocatalytic process has been found to be very active in the treatment of wastewater for the mineralization of broad range of organic pollutants. Nowadays, considerable attention has been paid to developing new photocatalytic materials, which is motivated largely by a demand for solving pollution problems.

As a new kind of photocatalytic materials, metal-organic frameworks (MOFs) have attracted much attention in purifying water by thoroughly decomposing organic matter[1–5] for their high surface area, strong mechanical stability, extraordinary porosity and designable architecture.[6–11] The continuing interest of MOFs as photocatalysts is due to the presence of organic linkers and central transition metal atoms, resulting in different charge-transfer transitions between ligands and metals, which make MOFs as potentially tunable photocatalysts. By choosing different types of metal ions and ligands, MOFs with different band sizes could be constructed and show good photocatalytic activity under irradiation.

MOFs that show good catalytic performance under irradiation could be obtained. It was reported that, under visible-light irradiation, Ti-benzenedicarboxylate [MIL-125(Ti)], amino-functionalized Ti-benzenedicarboxylate [NH_2-MIL-125(Ti)], Fe-benzenedicarboxylate [MIL-53(Fe)],[12,13] g-C_3N_4/Ti-benzenedicarboxylate (MIL-125(Ti), Ni-doped NH_2-MIL-125(Ti), $\{Na_6(H_2O)_{12}[Fe^{II}_2]_2[Fe^{III}_4(PO_4)][Fe^{II}(Mo_6O_{15})_2(PO_4)_8]_2\}(OH)_3\cdot 33H_2O$, $Bi_{25}FeO_{40}$/MIL-101(Cr)/PTH, ZnTCPc/UIO-66(NH_2) (ZnTCPc = zinc phthalocyanine), and MIL-68(In)-NH2/GrO were synthesized, and they all displayed excellent photocatalytic activities.[14–19] $[Zn(TBTC)(2,6\text{-pydc})]_n$ (HTBTC = 4,5,9,14-tetraaza-benzo[b]triphenylene-11-carboxylicacid, pydc = pyridine-2,6-dicarboxylic acid) showed an excellent photocatalytic activity for orange G and the rate of photodegradation for MV (methyl violet) can reach 90 % under Xe lamp irradiation after 4.5 h.[20] In addition, under UV light irradiation, $[Cd(TDC)(bix)(H_2O)]_n$ (H_2TDC = thiophene-2,5-dicarboxylic acid; bix = 1,4-bis(imidazol-1-ylmethyl)benzene)],[21] $[Mn_2L(1,10\text{-phen})_2]\cdot DMF\cdot 0.5H_2O$, $[Mn(1,10\text{-phen})(SO_4)(H_2O)_2]$ (H_4L = bis(3,5-dicarboxypheny1) terephthalamide),[22] and $[Cu_5(H_2L)_2(btb)_2(OH)_2]\cdot 3H_2O$ [H_6L = 2,4,6-trimethylbenzene-1,3,5-tris(methylenephosphonic acid); btb = 1,4-bis(1,2,4-triazol-1-yl)butane][23] were prepared, which showed good photocatalytic activities.

Moreover, bismuth is an environmentally friendly element, thus a number of bismuth-based MOFs with catalytic activity were investigated. For example, *G. Z. Wang*[24] synthesized a visible-light-responsive bismuth-based metal-organic framework (Bi-mna) (H_2mna = 2-mercaptonicotinic acid), which showed good photoelectric and photocatalytic properties. A bismuth-based fluorine-containing metal-organic framework $[Bi(OOCC_6F_5)_3(C_{10}H_8N_2)(H_2O)_2]$ ($OOCC_6F_5$ = pentafluorobenzoate, $C_{10}H_8N_2$ = 2,2′-bipyridine) was prepared by a hydrothermal method, which showed excellent properties of degrading Congo red in the presence of UV/Vis radiation.[25] In addition, the composites Bi_2WO_6/UiO-66 (UiO-66 = a zirconium based MOF)[26] and $BiVO_4$/MIL-101(Cr)[27] were also synthesized and they exhibited enhanced photocatalytic activity under visible-light irradiation.

In general, the photocatalysts based on MOFs have greatly developed. However, the preparation and synthetic of efficient MOFs photocatalysts still need to be investigated.

* Prof. Dr. Z.-X. Wei
E-Mail: zx_wei@126.com
* Prof. Dr. J.-F. Song
E-Mail: jfsong0129@nuc.edu.cn
[a] Department of Chemistry
School of Science
3 Xueyuan Road
Taiyuan, Shanxi, 030051, P. R. China
[b] Department of Safety Science and Engineering
Chemical Engineering and Environment Institute
3 Xueyuan Road
Taiyuan, Shanxi, 030051, P. R. China
Supporting information for this article is available on the WWW under **http://dx.doi.org/10.1002/zaac.201700096** or from the author.

1,3,5-Benzenetricarboxylic acid (H_3BTC) is usually used as organic ligand in the construction of MOFs. Considering the environmentally friendly character of bismuth element, the synthesis of MOFs based bismuth and H_3BTC by a hydrothermal method and its photocatalytic performance was investigated, and its structure was characterized. Compared with the reported [Bi(BTC)(DMF)]·DMF(CH_3OH)$_2$(Bi–BTC) though dimethylformamide (DMF),[28] the structure of the prepared Bi-based MOFs is different from the one reported in the literature.

Results and Discussion

Structural Description of {[Bi(BTC)(H_2O)$_2$]·H_2O}$_n$

Single-crystal X-ray diffraction analysis reveals that complex {[Bi(BTC)(H_2O)$_2$]·H_2O}$_n$ crystallizes in the monoclinic system, space group $P2_1/c$ and features a 3D metal-organic framework with Bi_2 secondary building units. Its asymmetric unit contains one central Bi^{3+} ion, one BTC^{3-} anion, two coordinated and one lattice water molecules. The Bi^{3+} ion is coordinated with nine oxygen atoms from four different BTC^{3-} anions and two coordinated water molecules (O2w and O3w), leading to a distorted monocapped square-antiprism coordination arrangement (Figure 1a). The distance of the Bi–O bonds range from 2.385(4) to 2.775(4) Å and the bond angles around Bi range from 49.12(7)° to 160.72(6)°. Two carboxylate groups of the BTC^{3-} anions coordinate with the Bi^{3+} cation in a bidentate chelate mode and the other coordinates in a mixture of both mono-dentate bridging and bidentate chelate modes (Figure 1b).

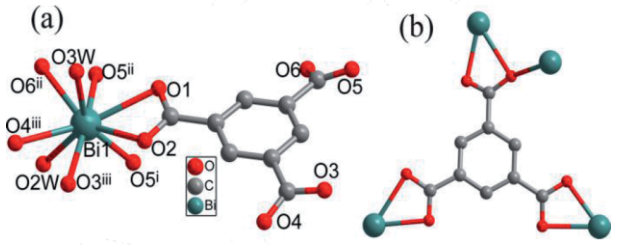

Figure 1. (a) Coordination environment of central Bi^{III} atoms in the crystal structure. Symmetry code: (i) 2–*x*, 0.5+*y*, 1.5–*z*; (ii) 1–*x*, 0.5+*y*, 1.5–*z*; (iii) *x*, 1.5–*y*, 0.5+*z*. (b) BTC^{3-} anions in complex {[Bi(BTC)(H_2O)$_2$]·H_2O}$_n$. Hydrogen atoms are omitted for clarity.

As can be seen from Figure 2(a), two central Bi atoms are connected into a Bi_2 secondary building unit (SBU) through two carboxylate oxygen atoms from two different BTC^{3-} anions, and the corresponding distance of Bi···Bi is 4.4883(3) Å. Each Bi_2 unit interconnected with six BTC^{3-} anions adopting μ_4-η^1: η^1: η^2 coordination modes into an interesting 3D metal-organic framework (Figure 2b). In the 3D framework, three central Bi atoms and three BTC^{3-} anions are interconnected into a ring with the dimension of 7.95×9.89 Å^2 (Figure S1, Supporting Information).

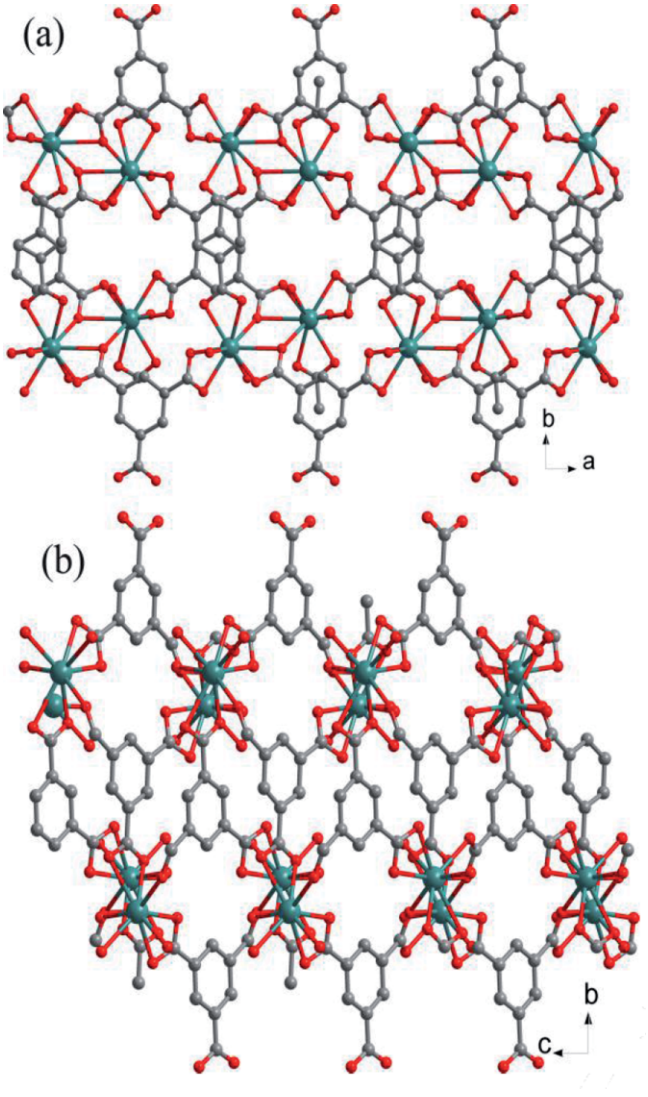

Figure 2. (a) 3D reticular structure along the *c* axis. (b) 3D pillar-layer framework of {[Bi(BTC)(H_2O)$_2$]·H_2O}$_n$ along the *a* axis direction. Hydrogen atoms and water molecules are omitted for clarity.

From the perspective of network topology, BTC^{3-} anions interacting with three Bi_2 units can be regarded as 3-connected nodes, and each Bi_2 unit interconnecting six BTC^{3-} can be all regarded as 6-connected nodes (Figure 3). So the framework

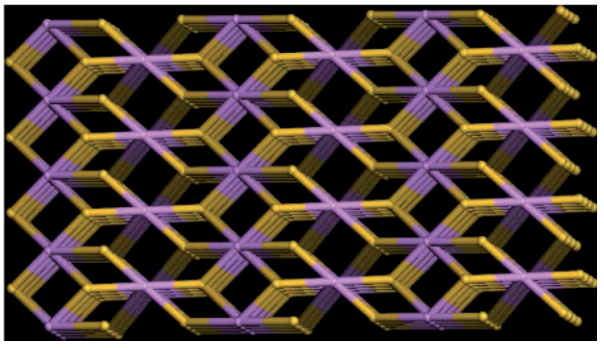

Figure 3. Topology network of complex {[Bi(BTC)(H_2O)$_2$]·H_2O}$_n$.

of compound may be simplified into a 2-nodal net with rtl rutile topology structure, as determined by TOPOS.[31]

X-ray Powder Diffraction of {[Bi(BTC)(H$_2$O)$_2$]·H$_2$O}$_n$

The X-ray powder diffraction pattern of complex was investigated in the solid state at room temperature (Figure 4). Powder X-ray diffraction was measured to determine the structure and purity of the sample. The peak positions simulated from the single-crystal X-ray data of complexes are in good agreement with those observed. A comparison of the experimental and simulated powder diffraction patterns confirms that the complex structures are solved accurately and the products are single phase.

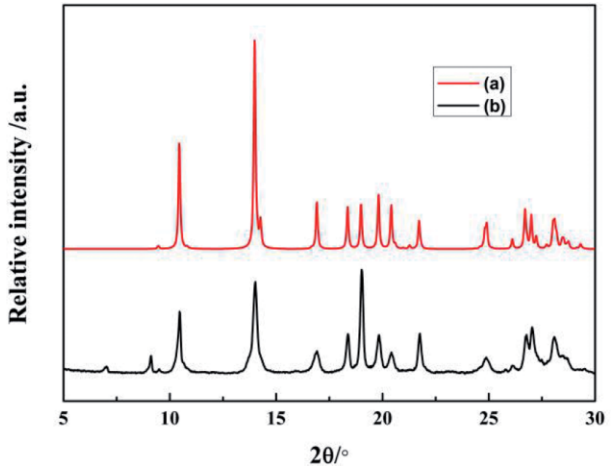

Figure 4. PXRD pattern of {[Bi(BTC)(H$_2$O)$_2$]·H$_2$O}$_n$: (a) simulated PXRD pattern; (b) experimental PXRD pattern.

IR Spectra of H$_3$BTC and of {[Bi(BTC)(H$_2$O)$_2$]·H$_2$O}$_n$

The IR spectrum of H$_3$BTC contains three characteristic peaks (Figure S2, Supporting Information): the stretching vibration of the carbonyl group (νC=O, 1721 cm^{-1}), the O–H stretching vibration of the carboxyl group (νO–H, 3100–2500 cm^{-1}), and the out-of-plane bending oscillation of hydroxyl group (δO–H, 918 cm^{-1}). The other two strong peaks located in 1404 and 1275 cm^{-1} are ascribed to in-plane bending vibration of hydroxyl group.[32]

In the IR spectrum of the complex {[Bi(BTC)(H$_2$O)$_2$]·H$_2$O}$_n$ (Figure S2, Supporting Information), the obvious absorption peak between 3680 cm^{-1} and 3120 cm^{-1} indicates the existence of H$_3$BTC. An apparent absorption peak also confirms the existence of COO$^-$ in the organic acid. The νC=O vibration and δO–H bending vibration of H$_3$BTC move from 1721 cm^{-1} and 918 cm^{-1} to 1608 cm^{-1} and 730 cm^{-1}, the peaks of νC=O and δO–H coupling zone at 1440–1395 cm^{-1} become wider, and the peaks at 1320–1210 cm^{-1} almost disappear, which proves that H$_3$BTC coordinates with metal ions.

UV/Vis Diffuse Reflectance Spectra (DRS) ofH$_3$BTC and {[Bi(BTC)(H$_2$O)$_2$]·H$_2$O}$_n$

The UV/Vis diffuse reflectance spectra (DRS) of H$_3$BTC and the complex {[Bi(BTC)(H$_2$O)$_2$]·H$_2$O}$_n$ are shown in Figure S3 (Supporting Information). Because of the same ligands, the shapes of the UV/Vis spectra of H$_3$BTC and complex {[Bi(BTC)(H$_2$O)$_2$]·H$_2$O}$_n$ are similar. The peak located at 233 nm is connected with electron transitions of π–π* from benzene rings. Then the weak peak is the result of charge-transfer LMCT (ligand-to-metal charge transfer) from ring to oxygen atom of the carboxy group. Compared with the ligand, the absorbance of the complex is strong. Obviously, the characteristic absorption bands of the complex have slight red shift: electron transitions of π–π* moves from 233 nm to 235 nm, charge-transfer LMCT moves from 324 nm to 332 nm, indicating the coordination of H$_3$BTC with bismuth. The ligand and the complex exhibited two absorption bands in the UV region of the spectrum. Clearly, the onset of the main optical absorption edges of {[Bi(BTC)(H$_2$O)$_2$]·H$_2$O}$_n$ is estimated to be 335 nm. Based on the relation E_g = 1240/λ,[13] the calculated optical bandgap of{[Bi(BTC)(H$_2$O)$_2$]·H$_2$O}$_n$ is 3.7 eV. The photoresponses of {[Bi(BTC)(H$_2$O)$_2$]·H$_2$O}$_n$ in the UV light region make them possess the potential capacity for photocatalytic reactions and the synthetic material is probably an ultraviolet light active photocatalyst.

Photoluminescence(PL) Spectra of H$_3$BTC and {[Bi(BTC)(H$_2$O)$_2$]·H$_2$O}$_n$

The photoluminescence spectra of H$_3$BTC and {[Bi(BTC)(H$_2$O)$_2$]·H$_2$O}$_n$ in solid state at room temperature are shown in Figure 5. H$_3$BTC exhibits an intense emission at 320 nm and two broad shoulders at 373 and 399 nm, which are attributed to the π*→π transition. Compared with H$_3$BTC, a red shift emission peak at 376 nm and the stronger broad shoulders of {[Bi(BTC)(H$_2$O)$_2$]·H$_2$O}$_n$ are exhibited. A red shift to 398 and 418 nm is found as well, which is due to the change in the coordination environment. The change in the coordination environment is consistent with the results of DRS spectra. The intensity change for the broad emission at 388–470 nm is ascribed to the increase in ligand conformational rigidity after coordination with Bi^{3+} cations, which may decrease the non-

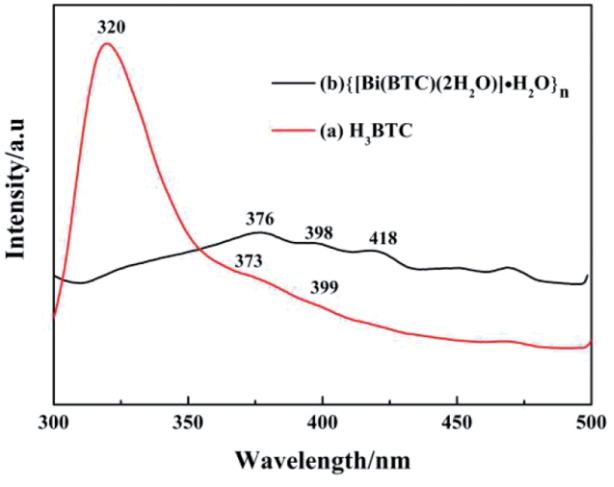

Figure 5. Photoluminescence spectra of (a) H$_3$BTC and (b) {[Bi(BTC)(H$_2$O)$_2$]·H$_2$O}$_n$ excited at 265 nm.

radiative transition of the excited state.[33] H_3BTC has a strong peak around 320 nm in the PL spectrum, which can be attributed to the bandgap recombination of electron-hole pairs. Comparatively, the PL intensity of $\{[Bi(BTC)(H_2O)_2]\cdot H_2O\}_n$ weakens significantly, suggesting that the recombination rate of the photo-generated electrons and holes slow down, indicating that the compound could have good photocatalytic activity.

Thermal Stability Study of $\{[Bi(BTC)(H_2O)_2]\cdot H_2O\}_n$

Thermogravimetric analysis experiments (TG-DSC) were performed on single crystal samples to determine thermal stability of the complex $\{[Bi(BTC)(H_2O)_2]\cdot H_2O\}_n$. Figure S4 (Supporting Information) shows the two weigh loss processes. The first weight loss (8.22 %) from 95 °C to 160 °C is corresponding to the loss of two coordination water molecules and one lattice water molecule (calcd. 11.43 %). The second weight loss from 345 °C to 456 °C can be attributed to the decomposition of organic ligands. It is corresponding to one endothermic peak and one exothermic peak in the DSC curve with peak temperatures at 119 and 388 °C, respectively. The complex completely converts to the remainder Bi_2O_3 with a residual weight of 60.45 %, which is basically corresponding to the calculated value 49.24 %. So the last product can be considered as Bi_2O_3.

Herein, the obtained complex decomposes at 388 °C, showing that $\{[Bi(BTC)(H_2O)_2]\cdot H_2O\}_n$ is stable to heat, and it can be a stable photocatalyst.

Photocatalytic Activity of $\{[Bi(BTC)(H_2O)_2]\cdot H_2O\}_n$ for Degradation of MO

The adsorption equilibrium could be reached when the catalyst was added into MO and was stirred in dark for 30 min. The adsorption equilibrium value was 1.0 % (Figure 6).

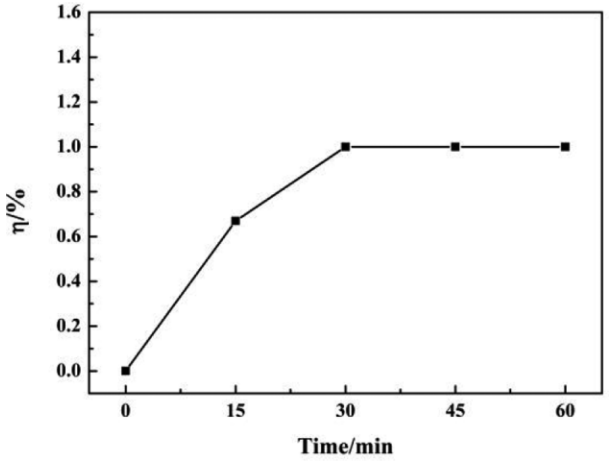

Figure 6. Adsorption of MO on $\{[Bi(BTC)(H_2O)_2]\cdot H_2O\}_n$.

The important factors, which influence photocatalytic activity, were also discussed. First, the effect of the pH value on the photocatalytic degradation of MO was investigated at room temperature. The solution pH was adjusted to 1.0, 3.0, 5.0, 7.0, 9.0, and 11.0 by using nitric acid and sodium hydroxide. As can be seen from Figure 7, when the pH of the MO solution was 3.0, the η % value reached 32.7 %, indicating that the optimum pH for the photocatalytic degradation of MO is 3.0.

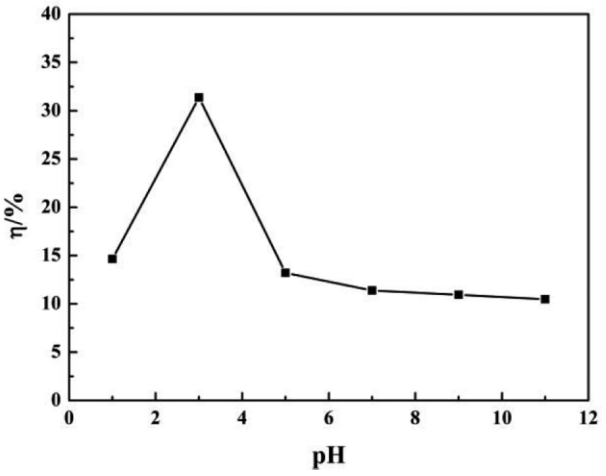

Figure 7. Effect of pH on photocatalytic degradation of MO.

The effect of the content of complex $\{[Bi(BTC)(H_2O)_2]\cdot H_2O\}_n$ on the photocatalytic degradation of MO when the pH was 3.0, is shown in Figure 8. The optimal value of the reaction catalyst was determined by changing the concentration from 0.05 $g\cdot L^{-1}$ to 1.00 $g\cdot L^{-1}$ to observe, which value can show best catalytic effect. When the amount of catalyst was less than 0.60 $g\cdot L^{-1}$, there was a relatively low degradation rate, and with the continuous increase of the amount of catalyst, the degradation rate improved and reached a maximum when the amount of catalyst was 0.60 $g\cdot L^{-1}$. However, the degradation rate began to reduce with increase of the amount of catalyst. This may be because too much catalyst would cover each other and affect the light absorption of the catalyst. Therefore, the optimal value of the catalyst content was 0.60 $g\cdot L^{-1}$.

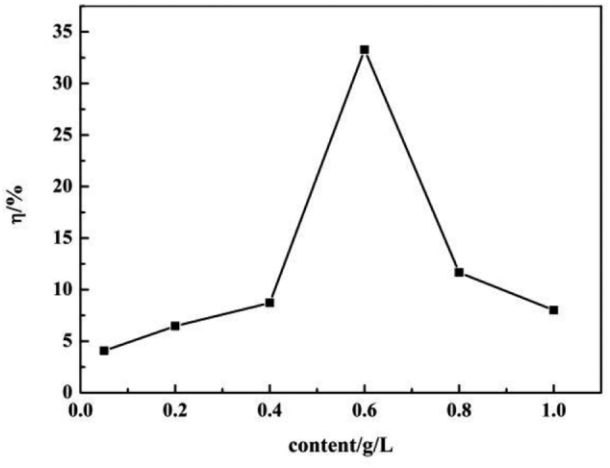

Figure 8. Effect of content of $\{[Bi(BTC)(H_2O)_2]\cdot H_2O\}_n$ on photocatalytic degradation of MO.

The effect of the reaction time on the photocatalytic degradation of MO when the pH value was 3.0 and the content of $\{[Bi(BTC)(H_2O)_2]\cdot H_2O\}_n$ was 0.60 $g\cdot L^{-1}$ is shown in Figure 9.

The catalytic effect improved with the extension of time and the photocatalytic reaction reached equilibrium when the reaction time was 60 min.

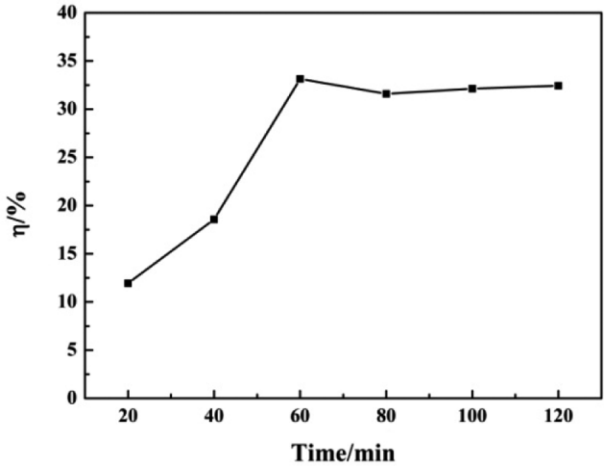

Figure 9. Effect of reaction time on photocatalytic degradation of MO.

Stability Experiments of {[Bi(BTC)(H$_2$O)$_2$]·H$_2$O}$_n$

The catalysis recycle experiment of {[Bi(BTC)(H$_2$O)$_2$]·H$_2$O}$_n$ was carried out when pH was 3.0 and the content of {[Bi(BTC)(H$_2$O)$_2$]·H$_2$O}$_n$ was 0.60 g·L^{-1}. To test its stability, we used one catalytic sample to conduct repetitive catalytic experiments. By changing the catalytic time from 1 h to 9 h, it was tested whether its structure changed. As can be seen from Figure S5 (Supporting Information), its structure kept consistent with the original one after the photocatalytic degradation of MO for 9 h, indicating that the catalyst is very stable under UV light.

The reported MOF prepared by an eco-friendly hydrothermal method was stable to heat and light, and showed certain photocatalytic activity under UV light. Other properties such as adsorption performance are under study in our laboratory.

Conclusions

A novel coordination complex {[Bi(BTC)(H$_2$O)$_2$]·H$_2$O}$_n$ was synthesized by an eco-friendly hydrothermal method and characterized. The complex crystallizes in the monoclinic $P2_1/c$ space group, a = 9.9077(4) Å, b = 16.9211(7) Å, c = 7.2357(3) Å, β = 109.513(1)°, and V = 1143.39(8) Å^3. When the pH value was 3.0, the content of {[Bi(BTC)(H$_2$O)$_2$]·H$_2$O}$_n$ was 0.60 g·L^{-1} and the catalytic time was 60 min, {[Bi(BTC)(H$_2$O)$_2$]·H$_2$O}$_n$ showed certain photocatalytic activity for the degradation of MO. In addition, the complex is decomposed at over 388 °C and it can maintain its structure after the photocatalytic degradation of MO for 9 h. Hence it is a stable ultraviolet light catalyst.

Experimental Section

Materials: All chemicals used were of analytical grade, and were used without further purification. H$_3$BTC was obtained from Aladdin industrial Corporation (Shanghai, China). Bismuth nitrate pentahydrate was supplied by Sinopharm Chemical Reagent Co., Ltd. (Shanghai,China).

Synthesis of {[Bi(BTC)(H$_2$O)$_2$]·H$_2$O}$_n$: The complex{[Bi(BTC)(H$_2$O)$_2$]·H$_2$O}$_n$ was prepared by an eco-friendly hydrothermal method with Bi(NO$_3$)$_3$·5H$_2$O and H$_3$BTC in distilled water. In a typical synthesis, Bi(NO$_3$)$_3$·5H$_2$O (0.194 g, 0.4 mmol) and H$_3$BTC (0.084 g, 0.4 mmol) were dissolved in distilled water (7.0 mL) in a 25.0 mL Teflon liner. After being stirred, the Teflon liner was sealed in a stainless steel autoclave and maintained at 130 °C for 72 h. The elongated needle-like crystallites were collected and washed with water. Yield: 35% (based on Bi). Before using the samples for the photocatalytic reactions, an activation process was performed on all bulk samples. In order to remove the guest molecules in the pores, the as-synthesized sample was stirred in distilled water for 3 h. Finally, the samples were filtered and dried under vacuum at 80 °C for 8 h.

X-ray Diffraction: X-ray single-crystal data was collected with a single-crystal Rigaku Mercury-CCD diffractometer equipped with a graphite-monochromated Mo-K_α radiation source (λ = 0.71073 Å) at 293 K. All absorption corrections were performed using the CrystalClear programs.[29] All structures were solved by the direct methods and refined by full-matrix least-squares fitting on F^2 by SHELXTL-97.[30] All non-hydrogen atoms were refined with anisotropic displacement parameters. All C-bound hydrogen atoms were refined using a riding model. The hydrogen atoms of water molecules were not located in a difference Fourier map in compound.

Crystallographic data (excluding structure factors) for the structure in this paper have been deposited with the Cambridge Crystallographic Data Centre, CCDC, 12 Union Road, Cambridge CB21EZ, UK. Copies of the data can be obtained free of charge on quoting the depository number CCDC-1508973 for {[Bi(BTC)(H$_2$O)$_2$]·H$_2$O}$_n$ (Fax: +44-1223-336-033; E-Mail: deposit@ccdc.cam.ac.uk, http://www.ccdc.cam.ac.uk).

Characterization: Infrared (IR) spectra were obtained as KBr Pellets with a PerkinElmer Spectrum One FT-IR spectrometer in the range of 4000–500 cm^{-1}. The UV/Vis diffuse reflectance spectra (DRS) for powder samples were recorded with a Thermo Evolution 220 equipped with an integrating sphere by using BaSO$_4$ as a white standard, whereas the UV/Vis spectra for solution samples were obtained with a Shimadzu UV 2550 spectrometer. XRD patterns were carried out with a Bruker D8 Advance X-ray diffractometer operated at 40 kV and 40 mA with Ni-filtered Cu K_a irradiation (λ = 0.15406 nm). The data were recorded in the 2θ range of 5–30°. Photoluminescence (PL) excitation and emission spectra were recorded with a Jobin Yvon Fluoro Max-4 spectrophotometer, which was equipped with a 150 W xenon lamp whose λ_{ex} was 265 nm as the excitation source at room temperature. Thermogravimetric analyses were performed with a NETZSCH STA 409PC differential thermal analyzer in a nitrogen atmosphere with a heating rate of 10 K·min from 30 to 800 °C. Photodegradation of the sample was surveyed by measuring the absorbance of the solution with a UV/visible spectrophotometer (Model 721, Shanghai Precision Scientific Instrument Co. Ltd, P. R. China).

Photocatalytic Studies: The photocatalytic experiment of MO aqueous was carried out at room temperature in a 100 mL watch glass containing a certain amount of photocatalyst and MO aqueous (10.0 mg·L^{-1}).The pH values of reaction solutions were adjusted with HNO$_3$ or NaOH. The mixture solution was stirred in dark for 30 min to achieve adsorption-desorption equilibrium between MO and the photocatalyst. After that the suspensions were irradiated by a 120 W UV lamp (Philips, 365 nm). After illumination, a suspension (about

2.0 mL) was taken from the reactor and centrifuged to separate the photocatalyst and MO solution. The concentration of MO solution was determined by UV/visible spectrophotometer (Model 721, Shanghai Precision Scientific Instrument Co. Ltd, P. R. China) at λ(max) = 464 nm using the standard curve. Adsorption and photocatalytic conversion (η %) was calculated as follows:

$$\eta\ \% = (C_0 - C_t)/C_0 \times 100\,\%$$

where C_0 and C_t (mg·L^{-1}) were the concentration of MO solution before and after the photocatalytic degradation, respectively.

Supporting Information (see footnote on the first page of this article): Details on the crystal structure analysis, IR and UV/Vis spectra, TG-DSC curves.

Acknowledgements

This work was supported by the National Natural Science Foundation of China (Nos. 21371159, 21201155, and 120247–13) and Technology Item in Taiyuan Shanxi (No. 120247–13).

Keywords: Hydrothermal method; Bismuth; Benzenetricarboxylic acid; Photocatalysis; Methyl orange (MO)

References

[1] H. Qu, L. Qiu, X. K. Leng, M. M. Wang, S. M. Lan, L. L. Wen, D. F. Li, *Inorg. Chem. Commun.* **2011**, *14*, 1347–1351.
[2] W. Q. Kan, B. Liu, J. Yang, Y. Y. Liu, J. F. Ma, *Cryst. Growth Des.* **2012**, *12*, 2288–2298.
[3] M. Y. Yoon, R. Srirambalaji, K. Kim, *Chem. Rev.* **2012**, *112*, 1196–1231.
[4] C. C. Chen, W. H. Ma, J. C. Zhao, *Chem. Soc. Rev.* **2010**, *39*, 4206–4219.
[5] F. Q. Wang, C. F. Dong, C. M. Wang, Z. C. Yu, S. K. Guo, Z. C. Wang, Y. N. Zhao, G. D. Li, *New J. Chem.* **2015**, *39*, 4437–4444.
[6] J. Guo, J. Yang, Y. Y. Liu, J. Fang Ma, *CrystEngComm* **2012**, *14*, 6609–6617.
[7] X. X. Xu, Z. P. Cui, J. Qi, X. X. Liu, *Dalton Trans.* **2013**, *42*, 4031–4039.
[8] L. Luo, P. A. Maggard, *Cryst. Growth Des.* **2013**, *13*, 5282–5288.
[9] T. Wen, D. X. Zhang, J. Zhang, *Inorg. Chem.* **2013**, *52*, 12–14.
[10] Y. Q. Chen, S. J. Liu, Y. W. Li, G. R. Li, K. H. He, Y. K. Qu, T. L. Hu, X. H. Bu, *Cryst. Growth Des.* **2012**, *12*, 5426–5431.
[11] J. Burt, W. Grantham, W. Levason, M. E. Light, G. Reid, *Polyhedron* **2015**, *85*, 530–536.
[12] R. W. Liang, F. F. Jing, L. J. Shen, N. Qin, L. Wu, *J. Hazard. Mater.* **2015**, *241*, 364–372.
[13] H. Wang, X. Z. Yuan, Y. Wu, G. M. Zeng, X. H. Chen, L. J. Leng, Z. B. Wu, L. B. Jiang, H. Li, *J. Hazard. Mater.* **2015**, *286*, 187–194.
[14] H. Wang, X. Z. Yuan, Y. Wu, G. M. Zeng, X. H. Chen, L. J. Leng, H. Li, *Appl. Catal. B Environ.* **2015**, *174–175*, 445–454.
[15] Y. H. Fu, L. Sun, H. Yang, L. Xu, F. M. Zhang, W. D. Zhu, *Appl. Catal. B Environ.* **2016**, *187*, 212–217.
[16] W. Zhu, X. Y. Yang, Y. H. Li, J. P. Li, D. Wu, Y. Gao, F. Y. Yi, *Inorg. Chem. Commun.* **2014**, *49*, 159–162.
[17] M. M. Lv, H. B. Yang, Y. L. Xu, Q. Chen, X. T. Liu, F. Y. Wei, *J. Environ. Chem. Eng.* **2015**, *3*, 1003–1008.
[18] C. Yang, X. You,J. H. Cheng,H. D. Zheng, Y. C. Chen, *Appl. Catal. B Environ.* **2017**, *200*, 673–680.
[19] Q. Liang, M. Zhang, Z. H. Zhang, C. H. Liu, S. Xu, Z. Y. Li, *J. Alloys Compd.* **2017**, *690*, 123–130.
[20] C. B. Liu, Y. Cong, H. Y. Sun, G. B. Che, *Inorg. Chem. Commun.* **2014**, *47*, 71–74.
[21] C. Y. Zhang, W. X. Ma, M. Y. Wang, X. J. Yang, X. Y. Xu, *Spectrochim. Acta Part A* **2014**, *118*, 657–662.
[22] F. Q. Wang, C. M. Wang, Z. C. Yu, K. H. Xu, X. Y. Li, Y. Y. Fu, *Polyhedron* **2016**, *135*, 49–55.
[23] S. Zhou, Z. G. Kong, Q. W. Wang, C. B. Li, *Inorg. Chem. Commun.* **2012**, *25*, 1–4.
[24] G. Z. Wang, Q. L. Sun, Y. Y. Liu, B. B. Huang, Y. Dai, X. Y. Zhang, X. Y. Qin, *Chem. Eur. J.* **2014**, *20*, 1–5.
[25] Y. J. Kong, L. J. Han, L. T. Fan, F. Z. Kong, *J. Fluorine Chem.* **2016**, *186*, 40–44.
[26] Z. Sha, J. L. Sun, H. Sze On Chan, S. Jaenicke, J. S. Wu, *RSC Adv.* **2014**, *4*, 64977–64984.
[27] Y. L. Xu, M. M. Lv, H. B. Yang, Q. Chen, X. T. Liu, F. Y. Wei, *RSC Adv.* **2015**, *5*, 43473–43479.
[28] G. Z. Wang, Y. Y. Liu, B. B. Huang, X. Y. Qin, X. Y. Zhang, Y. Dai, *Dalton Trans.* **2015**, 44:16238–16241.
[29] Molecular Structure Corporation & Rigaku, *CrystalClear*, Version 1.36. MSC, 9009 New Trails Drive, The Woodlands, TX 77381–5209, USA, and Rigaku Corporation, 3–9-12 Akishima, Tokyo, Japan, **2000**.
[30] R. P. Thummel, V. Goulle, B. Chen, *Org. Chem.* **1989**, *54*, 3057–3061.
[31] V. A. Blatov, A. P. Shevchenko, V. N. Serezhkin, *TOPOS3.2*, A new version of the program package for multipurpose crystal-chemical analysis, *J. Appl. Crystallogr.* **2000**, *33*, 1193.
[32] G. R. Liang, Y. R. Liu, X. Zhang, Z. X. Wei, *Synth. React. Inorg. Met. Org. Chem.* **2015**, *46*, 251–256.
[33] R.-S. Liu, V. Drozd, N. Bagkar, C.-C. Shen, I. Baginskiy, C.-H. Chen, C. H. Tan, *J. Electrochem. Soc.* **2008**, *155*, 71–73.

Received: March 28, 2017

Journal of Inorganic and General Chemistry
ZAAC
Zeitschrift für anorganische und allgemeine Chemie

ARTICLE

Z.-X. Wei, F. Ye, J.-F. Song,* X.-H. Wu, P. Yue* **1–7**

Synthesis, Characterization, and Photocatalytic Properties of Bismuth (III)-benzene-1,3,5-tricarboxylate